Available online at www.sciencedirect.com
SCIENCE DIRECT®
Journal of Solid State Chemistry 177 (2004) 648–653
JOURNAL OF SOLID STATE CHEMISTRY
http://elsevier.com/locate/jssc

Solid-state ^{27}Al NMR investigation of thermal decomposition of $LiAlH_4$

J.W. Wiench,[a] V.P. Balema,[a,1] V.K. Pecharsky,[a,b] and M. Pruski[a,*]

[a] *Ames Laboratory-USDOE, Iowa State University, Ames, IA 50011-3020, USA*
[b] *Department of Materials Science and Engineering, Iowa State University, Ames IA 50011, USA*

Received 24 June 2003; received in revised form 31 July 2003; accepted 1 August 2003

Abstract

Solid-state nuclear magnetic resonance is used to study the thermal decomposition of lithium tetrahydroaluminate into metallic aluminum, hydrogen and trilithium hexahydroaluminate. Aluminum sites in $LiAlH_4$ and Li_3AlH_6 were characterized using static, magic angle spinning (MAS) and multiple-quantum MAS NMR. By applying the in situ NMR method, it has been demonstrated that melting is not a prerequisite for the decomposition of $LiAlH_4$. Based on the observed data, a decomposition path has been established that is consistent with the concentrations of observed Al species at various stages of the thermally induced reaction. Published by Elsevier Inc.

Keywords: Hydrogen storage; Lithium tetrahydroaluminate; Trilithium hexahydroaluminate; Thermal decomposition of $LiAlH_4$; In situ NMR; ^{27}Al MAS NMR; ^{27}Al MQMAS NMR

1. Introduction

During the last decade, an increasing demand for high capacity sources of hydrogen compatible with modern fuel cell applications shifted the major emphasis in hydrogen storage research towards complex hydrides of light elements such as aluminum and boron [1,2]. Among the known aluminohydrides, two alkali metal derivatives containing more than 7% of hydrogen by weight, $LiAlH_4$ and $NaAlH_4$, have attracted particular attention [2]. Unlike other high-capacity hydrogen storage solids, such as magnesium hydride, pure lithium and sodium aluminohydrides release significant amounts of hydrogen at relatively low temperatures not exceeding 200°C. The use of an appropriate metal catalyst can lead to further reduction of their decomposition temperature all the way to room temperature [2–4].

The fundamental understanding of the processes taking place in solids during hydrogen release and uptake is very important for achieving further progress in applications of these materials for high capacity hydrogen storage. For several decades, the thermal decomposition of pure complex alkali metal tetrahydoaluminates, $MAlH_4$ where M = Li, Na, K or Cs, has been interpreted as a series of events, which begins with the melting of the hydride [5–7] and proceeds through the formation of an intermediate trialkali metal hexahydroaluminate M_3AlH_6:

$$MAlH_4(s) \rightarrow MAlH_4(l), \quad (1)$$

$$MAlH_4(l) \rightarrow \tfrac{1}{3} M_3AlH_6 + \tfrac{2}{3} Al + H_2, \quad (2)$$

$$\tfrac{1}{3} M_3AlH_6 \rightarrow MH + \tfrac{1}{3} Al + \tfrac{1}{2} H_2. \quad (3)$$

However, in the presence of an appropriate transition metal catalyst, both lithium and sodium tetrahydoaluminohydrides release hydrogen and transform into metallic aluminum and corresponding hexahydroaluminates at temperatures well below their melting points [2,4]. Hence, it is reasonable to assume that the decomposition of pure alkali metal aluminohydrides may follow several alternative routes, including ones that do not require the formation of a liquid phase. In this case, the role of the metal catalyst is to promote the low temperature decomposition path.

*Corresponding author. 230 Spedding Hall, Ames Laboratory, Ames, IA, 50011-3020, USA. Fax: +1-515-294-5233.
E-mail address: mpruski@iastate.edu (M. Pruski).
[1] Current address: Sigma-Aldrich Co. 5485, County Road V, Sheboygan Falls, WI 53085, USA.

0022-4596/$ - see front matter Published by Elsevier Inc.
doi:10.1016/j.jssc.2003.08.006

Recently, nuclear magnetic resonance (NMR) has been successfully employed for monitoring chemical transformations in solid complex aluminohydrides [3,8], where chemical reactions resulted in complete or partial amorphization of the samples and other analytical techniques, such as X-ray powder diffraction, could not provide sufficient structural information. In powdered solids containing quadrupolar nuclei such as ^{27}Al ($I = 5/2$), the NMR spectra are usually broadened by chemical shift anisotropy (CSA), dipolar, and quadrupolar interactions [9,10]. Broadening due to CSA and dipolar interactions can be eliminated by using magic angle spinning (MAS) combined with various decoupling strategies [9–11]. The quadrupolar effect can be overcome by employing a two-dimensional multiple quantum method combined with MAS (MQMAS) [12,13]. In the present study, we combine these high-resolution techniques with variable temperature (VT) in situ NMR of static samples to detail the mechanism responsible for the thermal decomposition of pure $LiAlH_4$.

2. Experimental

2.1. Sample preparation

$LiAlH_4$ (97% purity) was purchased from Fluka. Li_3AlH_6 was prepared from $LiAlH_4$ and LiH (Aldrich, 95% purity) as described in Ref. [14]. All operations on metal hydrides were carried out in a glove box under helium.

2.2. NMR measurements

The ^{27}Al NMR spectra were collected at 9.4 T on a Varian/Chemagnetics *Infinity* 400 spectrometer, operating at 104.24 and 400.02 MHz for ^{27}Al and ^{1}H, respectively. The spectrometer was equipped with a VT unit and doubly tuned MAS probes that use 5-mm (8 kHz MAS rate) and 3.2-mm (20 kHz MAS rate) zirconia rotors. Since the spin–spin relaxation times (T_1), as determined by saturation method, were 1.7, 1.3, and 1.0 s for $LiAlH_4$, Li_3AlH_6 and metallic aluminum, respectively, a pulse delay of 10 s was used in all experiments in order to detect fully equilibrated ^{27}Al magnetization. ^{1}H decoupling was accomplished by using the two-pulse phase modulation (TPPM) scheme [11,13], which performed better than the cw method under MAS conditions.

The MQMAS experiment utilized the Z-filter method [15] with the RF fields of ~170 and ~17 kHz during the excitation/conversion and selective Z-filter pulses, respectively. The t_1 step of 50 μs for data acquisition in F1 domain was synchronized with the spinning rate of the rotor (20 kHz). Shearing and scaling of the MQMAS spectra were performed as described previously [16,17].

In situ VT NMR experiments on $LiAlH_4$ were performed using static (non-spinning) 5-mm glass tubes, which were loaded under helium in a glove box and sealed using a Teflon tape. The tape allowed for hydrogen gas to escape during heating. The measurements were carried out in a nitrogen flow to further minimize the possibility of oxygen contamination. The VT unit was calibrated using $Pb(NO_3)_2$ as a 'chemical shift thermometer', which allowed to establish the temperature of a sample under static and MAS conditions with the accuracy of ± 1°C [18]. The observed ^{207}Pb line width revealed that the temperature gradient across the sample did not exceed 1.5°C. The ^{27}Al spectra reported in this work use the δ scale, with positive values downfield, and are referenced to 1 M $Al(H_2O)_6^{3+}$ aqueous solution.

3. Results and discussion

The MAS and static ^{27}Al NMR spectra of pure $LiAlH_4$ are shown in Figs. 1a and b, respectively. In addition to the dominant resonance at around 100 ppm representing four-coordinated Al in $LiAlH_4$, the spectrum in Fig. 1a revealed minor amount of metallic aluminum (Al_M), whose chemical shift of 1640 ppm agrees with the literature data [19]. The corresponding NMR spectra of as-synthesized Li_3AlH_6 are shown in Figs. 1c and d. As expected, they feature a single resonance at approximately −30 ppm representing six-coordinated Al.

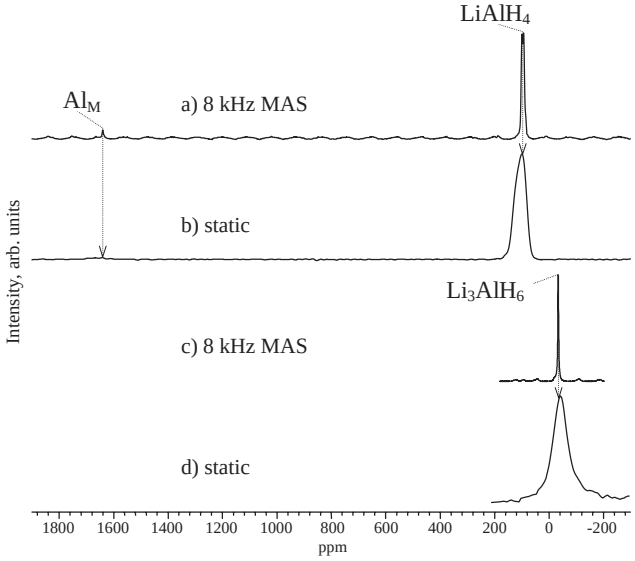

Fig. 1. ^{27}Al NMR spectra of $LiAlH_4$ (a,b) and Li_3AlH_6 (c,d) recorded using 8 kHz MAS (a,c) and static (b,d). All spectra were acquired at room temperature, using ^{1}H decoupling.

To facilitate the ensuing discussion of the mechanism of thermal decomposition, a separate set of experiments was performed to examine the width of observed ^{27}Al lines in $LiAlH_4$ under various conditions. The full-width at half-magnitude (FWHM) of the ^{27}Al signal of a static sample acquired under single pulse excitation is approximately 9.5 kHz (see Fig. 2a). The use of ^{1}H TPPM decoupling reduced the FWHM by a factor of almost two (Fig. 2b). The combination of MAS and ^{1}H decoupling (Fig. 2d) yielded further improvement and allowed for observation of well-defined powder pattern representing the central ($m = +1/2 \leftrightarrow m = -1/2$) transition of ^{27}Al nuclei which is broadened by the second-order quadrapolar interaction. The highest resolution in solid $LiAlH_4$ has been achieved by the method of MQMAS (Fig. 2e), which will be discussed in more detail below. Finally, Fig. 2f demonstrates the single-pulse ^{27}Al spectrum of molten $LiAlH_4$ acquired at 180°C. Due to increased mobility, the observed signal narrowed to 400 Hz, i.e., by a factor of almost 20 when compared with the spectrum of Fig. 2a.

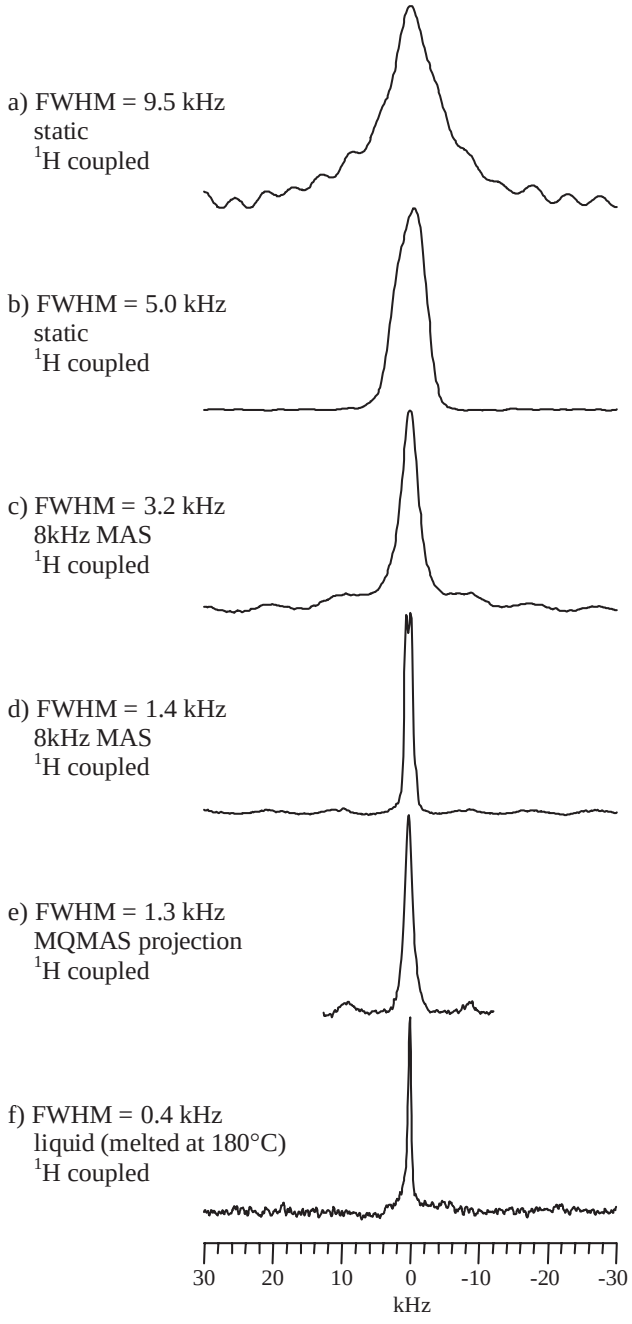

Fig. 2. ^{27}Al NMR lineshapes observed in $LiAlH_4$. Spectra (a)–(e) were acquired at room temperature, other experimental conditions are shown in the figure.

The ^{27}Al MAS and MQMAS spectra of $LiAlH_4$ acquired with the assistance of ^{1}H decoupling via TPPM [13,15] are shown in Fig. 3. The sheared MQMAS spectrum is presented as a two-dimensional correlation plot between single and triple quantum coherences. The single quantum dimension of the MQMAS spectrum (horizontal, δ_2) has the same resolution as the standard MAS spectrum. Note that MAS and MQMAS yielded somewhat different line shapes of the central transition powder pattern. This is due to the dependence of the MQ excitation and conversion on the crystallite orientation in a powdered sample, which skews the spectral intensities in the single quantum dimension [17]. The multiple quantum dimension (vertical, δ_{ISO})

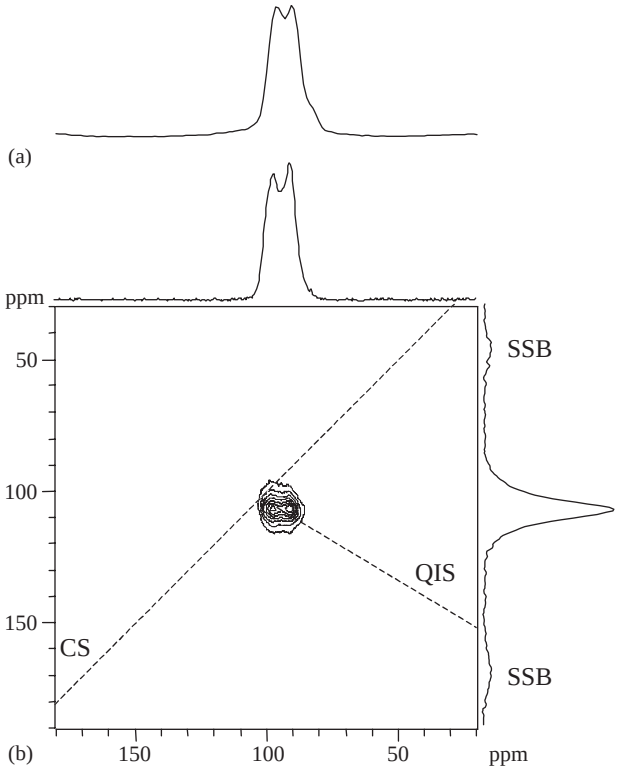

Fig. 3. (a) ^{27}Al spectrum of $LiAlH_4$ obtained under MAS at 8 kHz; (b) ^{27}Al MQMAS spectrum of $LiAlH_4$ obtained under MAS at 20 kHz. ^{1}H TPPM decoupling was used in both experiments. Chemical shift (CS) and quadrupole induced shift (QIS) axes are represented by dashed lines [17]. 'SSB' denotes the spinning sidebands.

Table 1
^{27}Al NMR parameters obtained for pure hydrides by QUASAR simulation of the MAS spectra

	δ_{iso} (ppm)	C_Q (MHz)	η_Q	$\Delta\delta_{CSA}$ (ppm)	η_{CSA}
$LiAlH_4$	103.8±0.8	3.9±0.1	0.24±0.05	30±10	0.0±0.1
Li_3AlH_6	−33.7±0.8	1.4±0.1	0.02±0.05	25±10	0.0±0.1

The following definitions were used: isotropic shift δ_{iso} is a sum of chemical shift (δ_{CS}) and quadrupole induced shift (δ_{QIS}), quadrupole coupling constant $C_Q = e^2qQ/h$; anisotropy of quadrupolar tensor $\eta_Q = (V_{yy} - V_{xx})/V_{xx}$; chemical shift anisotropy $\Delta\delta_{CSA} = 1.5(\delta_{33} - \delta_{CS})$; anisotropy of CSA $\eta_{CSA} = (\delta_{22} - \delta_{11})/(\delta_{33} - \delta_{CS})$, see Refs. [9,10,17] for details.

represents the isotropic resonance that is free from the second-order effects [12,17]. The numerical simulation of the MAS spectrum of Fig. 3a by QUASAR [20] and the standard analysis of MQMAS spectrum of Fig. 3b [17] yielded the same set of line shape parameters for the tetrahedral site in $LiAlH_4$, which are given in Table 1. The measured quadrupolar coupling constant C_Q of 3.9 MHz agrees with the previous NMR study [21]. The ^{27}Al MAS and sheared MQMAS NMR spectra of Li_3AlH_6 (not shown) exhibit a single symmetric resonance whose line parameters are consistent with the six-coordinated aluminum (see Table 1). The MQMAS spectra of $LiAlH_4$ and Li_3AlH_6 disclosed the presence of weak spinning sidebands due to the CSA interaction, which is magnified by a factor of p (in our approach $p = 3$) along the MQ dimension [17,22]. Our simulation yielded the CSA values of 30 and 25 ppm for $LiAlH_4$ and Li_3AlH_6, respectively.

The thermal decomposition of $LiAlH_4$ was studied in situ between 20°C and 150°C under static conditions, as described in the Experimental section (Fig. 4). After 30 min of exposure to 100°C, only trace amounts of metallic aluminum (Al_M) and Li_3AlH_6 were detected. At 150°C, however, the decomposition process accelerated significantly. Resonances representing Al_M, Li_3AlH_6, and a new peak at 60 ppm, which was assigned as six-coordinated oxidized Al^{III} derivative (abbreviated as Al_O), intensified at the expense of $LiAlH_4$, which disappeared almost completely within 2 h. The amount of Al_O increased further as a function of time, most likely due to a reaction of gaseous oxygen impurity with highly active metallic aluminum.

The estimated relative concentrations of various Al species during the thermal decomposition at 150°C are shown in Fig. 5. We note that the quantification of different aluminum species in the spectra of Fig. 5 is not straightforward [10,19]. First, the resonance assigned to $LiAlH_4$ is dominated by the central transition, and thus represents only 9/35 of the ^{27}Al resonance signal in this hydride [10]. The satellite transitions for this site appear as a wide manifold of spinning sidebands in the MAS spectrum of Fig. 1a. Similar effect is expected for Li_3AlH_6, although non-negligible contribution of the satellite transition intensity may be expected due to more symmetric coordination of Al in this compound. In contrast, the metallic aluminum has a cubic crystal

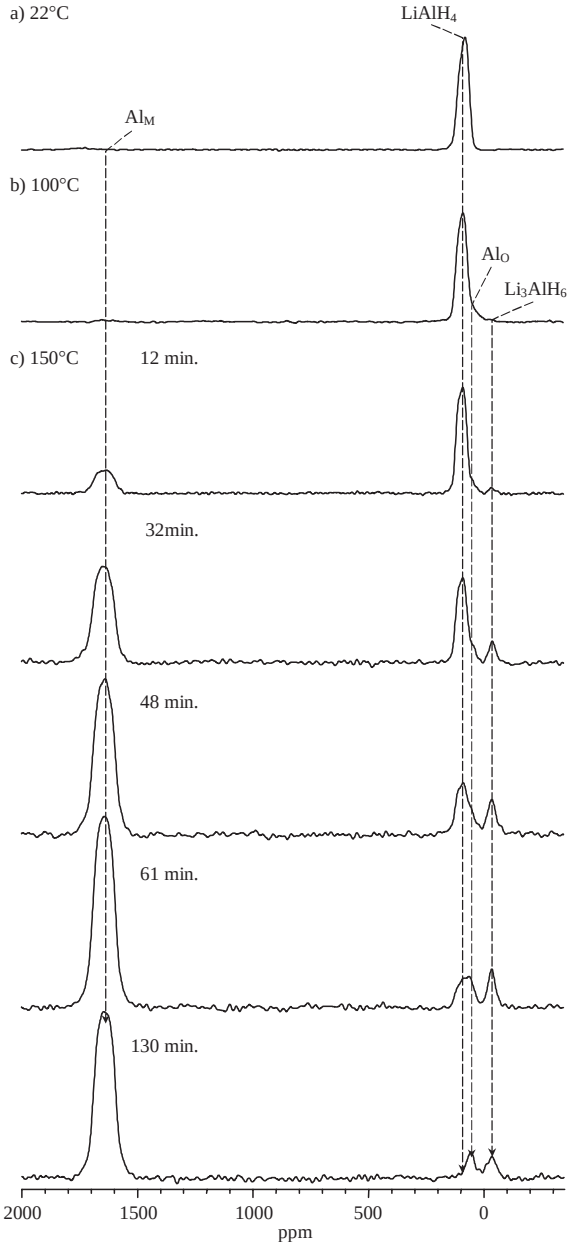

Fig. 4. ^{27}Al static spectra of $LiAlH_4$ measured under ^{1}H decoupling as a function of heating conditions.

structure, which leads to degeneracy of all the transitions [19]. Consequently, the entire intensity of the metal peak is accounted for in the resonance at 1640 ppm.

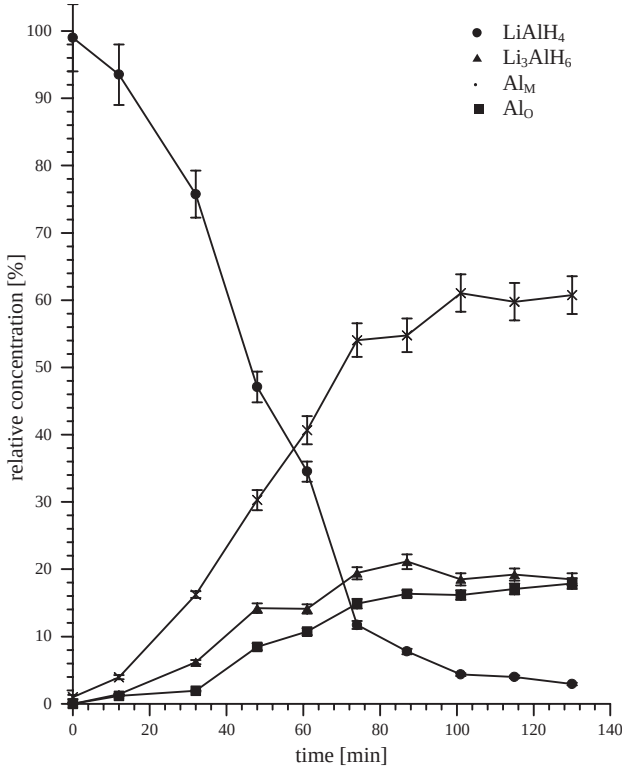

Fig. 5. Relative concentrations of the observed Al species versus exposure time at 150°C.

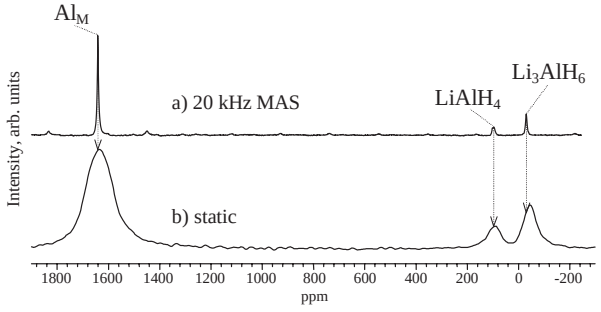

Fig. 6. ^{27}Al NMR spectra of 1:1:1 molar mixture of $LiAlH_4$, Li_3AlH_6 and Al_M obtained under ^{1}H decoupling using 20 kHz MAS (a) and static (b) conditions.

Second, the RF excitation and the probe tuning were optimized for the central transition of $LiAlH_4$, which had the opposite effect of reducing the intensity of the peak corresponding to metallic aluminum, as it was measured with a large resonance offset. In order to properly account for these effects, we took a static ^{27}Al NMR spectrum of the 1:1:1 molar mixture of $LiAlH_4$, Li_3AlH_6 and Al (see Fig. 6b). (We note that the MAS spectrum of the same mixture shown in Fig. 6a yielded the same relative intensities, provided that the spinning sidebands associated with Al were included in the calculation.) The obtained intensities were then used to calibrate the intensities of the spectra in Fig. 4.

Our NMR studies offer new insights into the mechanism of thermal decomposition, which deserve further discussion. First, while heating $LiAlH_4$ to 150°C caused disintegration of the hydride and the formation of Li_3AlH_6 and Al/Al_O, no line narrowing corresponding to the melting of $LiAlH_4$ (see Fig. 2e) could be detected. Instead, the observed ^{27}Al line widths are consistent with those measured in solid $LiAlH_4$, Li_3AlH_6 and Al_M (see Figs. 1, 2 and 6), which clearly demonstrates that undoped $LiAlH_4$ can decompose in the solid state, and its melting *is not* a prerequisite for this process. A possibility that thermal decomposition of $LiAlD_4$ may not require melting of the sample was also mentioned by Brinks et al. [23], who studied thermal transformations of $LiAlD_4$ using neutron and X-ray powder diffraction techniques. Second, the analysis of integral intensities of the signals in the ^{27}Al NMR spectrum of the decomposed sample (Fig. 5) reveals an apparent deviation of the sample composition from that predicted by Eq. (2). Indeed, the concentration of Li_3AlH_6 in the hydride sample after exposure to 150°C for 130 min was found to be ~18 mol% instead of the expected value of 33.3 mol% if the reaction proceeded according to Eq. (2). At the same time, it is well known that Li_3AlH_6 decomposes thermally at the temperatures far above 150°C [6,7,14]. Note that very little, if any, change in the concentration of Li_3AlH_6 (and other aluminum species) is observed in Fig. 5 after ~80 min at 150°C, i.e., when the decomposition of $LiAlH_4$ is practically completed. Therefore, the deviation from the expected stoichiometry as a result of the decomposition of trilithium hexahydroaluminate (Eq. (3)) is rather unlikely. Remarkably, gas-volumetric data on thermal decomposition of $LiAlH_4$ published by Dymova et al. [7] clearly support the results of our NMR studies. Based on the amount of hydrogen released by $LiAlH_4$ during its exposure to 150–200°C [7], the concentration of Li_3AlH_6 in the sample cannot exceed ~22 mol%, which disagrees with the stoichiometry represented by the Eq. (2) but it is in a fairly good agreement with our data.

4. Conclusion

Our studies on the thermal decomposition of lithium aluminohydride using in situ high-temperature solid-state ^{27}Al NMR spectroscopy revealed that undoped commercial $LiAlH_4$ can decompose at 150°C without melting, and the chemical composition of the sample kept at this temperature for 130 min does not agree with that expected for a two-step process suggested previously. Therefore, it seems feasible that thermal decomposition of lithium tetrahydroaluminate follows

several different reaction paths including that represented by

$$LiAlH_4 \rightarrow LiH + Al + \tfrac{3}{2}H_2. \quad (4)$$

Note that the transformation of $LiAlH_4$ directly into LiH, Al and H_2 is also feasible from the thermodynamic point of view [7].

Acknowledgments

Different aspects of this research were supported at Ames Laboratory by the US Department of Energy, Office of Basic Energy Sciences, Division of Chemical Sciences, and Division of Materials Sciences under Contract W-7405-Eng-82.

References

[1] M. Gardiner, Presented at the 224th ACS National Meeting, Boston, MA, United States, August 18–22, 2002.
[2] B. Bogdanovic, G. Sandrock, MRS Bull. 27 (2002) 712.
[3] V.P. Balema, J.W. Wiench, K.W. Dennis, M. Pruski, V.K. Pecharsky, J. Alloys Compd. 329 (2001) 108.
[4] V.P. Balema, K.W. Dennis, V.K. Pecharsky, Chem. Commun. 17 (2000) 1665.
[5] E.C. Ashby, Adv. Inorg. Chem. Radiochem. 8 (1966) 283.
[6] J.A. Dilts, E.C. Ashby, Inorg. Chem. 11 (1972) 1230.
[7] T.N. Dymova, V.N. Konoplev, D.P. Aleksandrov, A.S. Sizareva, T.A. Silina, Russ. J. Coord. Chem. 21 (1995) 165.
[8] B. Bogdanovic, M. Felderhoff, M. Germann, M. Hartel, A. Pommerin, F. Schuth, C. Weidenthaler, B. Zibrowius, J. Alloys Compd. 350 (2003) 246.
[9] A.-R. Grimmer, B. Blümich, NMR Basic Principles Progr. 30 (1994) 1.
[10] D. Freude, J. Haase, NMR Basic Principles Progr. 29 (1993) 1.
[11] A.E. Bennett, C.M. Rienstra, M. Auger, K.V. Lakshmi, R.G. Griffin, J. Chem. Phys. 103 (1995) 6951.
[12] L. Frydman, J.S. Harwood, J. Am. Chem. Soc. 117 (1995) 5367.
[13] V. Lacassagne, P. Florian, V. Montouillout, C. Gervais, F. Babonneau, D. Massiot, Magn. Reson. Chem. 36 (1998) 956.
[14] V.P. Balema, V.K. Pecharsky, K.W. Dennis, J. Alloys Compd. 313 (2000) 69.
[15] J.-P. Amoureux, C. Fernandez, S. Steuernageel, J. Magn. Reson. A 123 (1996) 116.
[16] D. Massiot, B. Touzo, D. Trumeau, J.P. Coutures, J. Virlet, P. Florian, P.J. Grandinetti, Solid State Nucl. Magn. Reson. 6 (1996) 73.
[17] J.-P. Amoureux, M. Pruski, in: D.M. Grant, R.K. Harris (Eds.), Encyclopedia of NMR, Vol. 9, John Wiley & Sons Ltd., Chicester, 2002, p. 226.
[18] A. Bielecki, D.P. Burum, J. Magn. Reson. A 116 (1995) 215.
[19] L. Kellberg, H. Bildsoe, H.J. Jakobsen, J. Chem. Soc. Chem. Commun. 19 (1990) 1294.
[20] J.-P. Amoureux, C. Fernandez, Y. Dumazy, Presented at the 37th Rocky Mountain Conference, Denver, CO, USA, July–August 1995.
[21] V.P. Tarasov, S.I. Bakum, S.F. Kuznetsova, Russ. J. Inorg. Chem. 42 (1997) 694.
[22] L. Marinelli, L. Frydman, Chem. Phys. Lett. 275 (1997) 188.
[23] H.W. Brinks, B.C. Hauback, P. Norby, H. Fjellvag, J. Alloys Compd. 351 (2003) 222.